

Expression, purification and functional analysis of an odorant binding protein AegOBP22 from *Aedes aegypti*

Gang Yang^{a,*}, Gösta Winberg^b, Hui Ren^b, Shuguang Zhang^b

^a Institute for Nanobiomedical Technology and Membrane Biology, Sichuan University, Keyuan 4 St., Gaopeng Avenue, Chengdu 610041, China

^b Center for Biomedical Engineering, NE47-379, Massachusetts Institute of Technology, 77 Massachusetts Avenue, Cambridge, MA 02139-4307, United States

ARTICLE INFO

Article history:

Received 14 July 2010
and in revised form 2 September 2010
Available online 7 September 2010

Keywords:

Aedes aegypti
Circular dichroism
Fluorescent probe
Odorant binding protein
Protein purification

ABSTRACT

Mosquitoes that act as disease vectors rely upon olfactory cues for host-seeking, mating, blood feeding and oviposition. To reduce the risk of infection in humans, one of the approaches focuses on mosquitoes' semiochemical system in the effort to disrupt undesirable host–insect interaction. Odorant binding proteins (OBPs) play a key role in mosquitoes' semiochemical system. Here, we report the successful expression, purification of an odorant binding protein AegOBP22 from *Aedes aegypti* in heterologous system. Protein purification methods were set up by Strep-Tactin affinity binding and size-exclusion chromatography. Analysis by SDS–PAGE and mass spectrum revealed the protein's purity and molecular weight. Circular dichroism spectra showed the AegOBP22 secondary structure had a pH dependent conformational change. The protein functions of AegOBP22 were tested by fluorescent probe 1-NPN binding assays and ligands competitive binding assays. The results show AegOBP22 proteins have characteristics of selective binding with various ligands.

© 2010 Elsevier Inc. All rights reserved.

Introduction

The success of host-seeking, mating, blood feeding and oviposition determine life history strategies of mosquitoes. Each of these behaviors is mediated by both internal and external factors. The most important external factor affecting mosquito behavior is olfactory cue. Many behavioral expressions of mosquitoes are mediated by olfaction [1,2]. For example, female *Anopheles gambiae* mosquitoes, which are the main vectors of malaria transmission in sub-Saharan Africa, use olfactory cues to find human hosts and avoid non-human hosts [3–6]. *Aedes aegypti* mosquitoes are carriers of dengue and yellow fever, using olfactory cues for foraging and oviposition [7,8]. To reduce the risk of infection in humans, one of the approaches focuses on the semiochemical systems of mosquitoes and other insects in the effort to disrupt undesirable host–insect interaction. Indeed, the chemical ecology of mosquitoes is now widely recognized as one area of investigation on which future vector-borne disease control strategies may depend [3,9].

Perception of volatile semiochemicals in mosquitoes is mediated, as for other insects, by chemosensory neurons segregated within specific olfactory sensilla located mainly on the antennae and maxillary palps [8,10,11]. These semiochemicals, such as pheromones, plant volatiles or animal odors are small hydrophobic

molecules which enter the antennae and other sensory organs via pores and pass across the hydrophilic sensilla lymph surrounding the olfactory neuronal dendrites. The sensilla lymph containing extremely high concentrations of odorant binding proteins (OBPs)¹, including the pheromone-binding proteins (PBP) and the so-called general odorant binding proteins (GOBPs), which solubilize and transport the odorant molecules from the porous cuticular surface of the antennal sensilla through the sensilla lymph to the G-protein-coupled odorant receptors (ORs) residing on the olfactory sensory neuron [12,13].

Considerable progress has been made in the field of olfaction with respect to mosquito–host interactions. The recent publications of *A. aegypti* OBPs and *A. gambiae* OBPs as well as ongoing sequencing projects of other important mosquito vectors offer new opportunities to advance our knowledge on mosquito olfaction [14]. *A. gambiae* and *A. aegypti* are two kinds of the most studied mosquito species. AgamOBP1 is one of OBPs found from the *A. gambiae*. By circular dichroism (CD) assays and AgamOBP1/bombykol ligand binding assays, Wogulis et al. found the conformational change of AgamOBP1 led to a significant loss of ligand affinity capacity when pH dropped from 7.0 down to 5.5 [3]. Li et al. identified the recombinant protein *A. aegypti* OBP22 could bind to a variety of chemical odors containing one or two benzene

* Corresponding author.

E-mail addresses: yanggangscu@gmail.com (G. Yang), shuguang@mit.edu (S. Zhang).

¹ Abbreviations used: OBPs, odorant binding proteins; PBPs, pheromone-binding proteins; GOBPs, general odorant binding proteins; ORs, odorant receptors; CD, circular dichroism; MW, molecular weight; CVs, column volumes.

ring structures [7]. These characteristics of selective binding of various ligands widely exist in mosquito OBPs and the OBPs of *Drosophila melanogaster*, honeybee, locusts and rat [1,15–17].

In our recent studies, we focused on developing a heterologous system for producing OBPs, and studied the functions of the AegOBP22. In this article, we report the successful expression, purification of AegOBP22 by the way of *Escherichia coli* extracellular secretion. Protein purification methods were set up by Strep-Tactin affinity binding and size-exclusion chromatography. Analysis by SDS-PAGE and mass spectrum revealed those protein purify and molecular weight (MW). CD spectra showed the AegOBP22 underwent a pH dependent conformational change of secondary structure. The protein functions of AegOBP22 were tested by fluorescent probe 1-NPN binding assays and ligands competitive binding assays. The results show AegOBP22 proteins have characteristics of selective binding with various ligands.

Our work provides a new approach to study OBPs; it will enhance the understanding of mosquitoes' semiochemical system and develop new disease control strategies against mosquitoes. Moreover, our work will likely facilitate the design of bionic artificial nose based on nano-bio devices for a wide range of applications, from detection of infinitesimal amounts of odors, emitted from diverse diseases and environment to develop artificial organs.

Materials and methods

Reagents and buffers

All common chemicals were obtained from either Sigma (St. Louis, MO) or VWR International unless otherwise indicated. Liquid growth medium used for *E. coli* culture was Luria-Bertani (LB) medium. SDS-PAGE gels and protein standards were purchased from Invitrogen (Carlsbad, CA). Protein purification materials were purchased from GE Healthcare Life sciences (Uppsala, Sweden).

Buffer for *E. coli* culture (KPO₄ buffer): 940 ml 1 M K₂HPO₄ + 60 ml 1 M KH₂PO₄, pH 8.0. Buffers for Strep-Tactin column: (1) buffer W1: 100 mM Tris-Cl pH 9.0, 150 mM NaCl, 1 mM EDTA, 1 mM DTT; (2) buffer W2: buffer W1 + 0.2% Triton-X-114; (3) buffer E: buffer W1 + 2.5 mM desthiobiotin. Buffer for S200 gel filtration column (buffer S): 1×PBS buffer.

AegOBP22 heterologous expression

AegOBP22 (GenBank accession no. EAT42725) gene was selected from GenBank. The plasmids with AegOBP22 gene were customized and ordered from GENEART (Germany). The vector backbone of the gene is pET28a (+).

The AegOBP22 plasmids were transformed into BL21(DE3)-STAR-pLysS competent cells, then the cells were spread on LB-agar plates, followed by overnight culture at 37 °C. The colonies from LB-agar plates were selected and cultured in 5 ml of LB liquid medium, plus 50 µl of 50% glucose, overnight at 37 °C with shaking. The next morning, 1 ml of overnight culture was inoculated in 100 ml of fresh LB liquid medium, plus 1 ml of 50% glucose, and cell culture was continued at 37 °C with shaking while monitoring growth of the culture by measuring the optical density at 600 nm (OD₆₀₀). At OD₆₀₀ of 0.6–0.8, 100 ml of culture was inoculated into 3 L LB, plus 30 ml of 50% glucose and 90 ml KPO₄ buffer. The cell culture was continued again at 37 °C with shaking while monitoring growth of the culture. Once OD₆₀₀ reached 0.6 again, the temperature was decreased to 16 °C and after 20 min, the inducer was added (1 mM IPTG). The concentration was monitored every 2 h until harvested at 16 h post induction. All plates and LB liquid media used here contained 25 µg/ml of kanamycin.

The harvested media were centrifuged at 10,000 rpm at 4 °C for 1 h in Avanti J-E (Beckman); decanted supernatant; corrected pH to 9.0 by adding 1 M NaOH while stirring the supernatant; added 100 mM PMSF and 100 µg/ml ampicillin; kept at 4 °C.

AegOBP22 protein purification

Before loading on Strep-Tactin column, the supernatant was added 0.2% TritonX-114 and filtered by using a 0.22 µm filter. The Strep-Tactin column contained 10 ml Strep-Tactin beads (IBA BioTAGnology, Germany). The supernatant was loaded on the Strep-Tactin column by a peristaltic pump at a rate of 2 ml/min at +4 °C cold room. After loading, the Strep-Tactin column was washed with 5 column volumes (CVs) of wash buffer W1, and continued with 5 CVs wash buffer W2. For eluting the target proteins, the Strep-Tactin column was connected to an Äkta Purifier HPLC system (GE Healthcare). The target proteins were eluted with buffer E over 5 CVs.

The elution fractions were tested by SDS-PAGE via Coomassie blue staining. Those containing OBPs were pooled and concentrated by using a 10 kDa MWCO filter column (Millipore, USA). To improve the purity of the protein, the concentrated proteins were subjected to size-exclusion chromatography by using a Hi-Load 16/120 Superdex 200 column (Amersham Pharmacia Biosciences). The column was preequilibrated with buffer S. After loading, the column was run with buffer S at 1 ml/min and column flowthrough was monitored via UV absorbance at 280 nm and 215 nm. Protein fractions were collected using an automated fraction collector. Peak fractions were then pooled, concentrated and subjected to SDS-PAGE test. The concentration of purified proteins was determined by a NanoDrop ND-1000 spectrophotometer (Thermo Scientific, USA).

Mass spectrometric analysis

The mass spectrum was generated from a sample of AegOBP22 monomer. MW measurements were made by LC-MS with MIT Koch Institute Proteomics Facility's QSTAR Elite quadrupole-time-of-flight mass spectrometer.

Circular dichroism (CD) detection

The purified protein samples came from gel filtration fractions and were concentrated to 6.3 mg/ml. In order to study the secondary structural change of AegOBP22 in different pH environment, a small amount of the concentrated AegOBP22 were diluted with PBS of different pH, from 5.0 to 9.0. The final AegOBP22 concentration using for CD experiments was 0.2 mg/ml, about 12 µM of AegOBP22 proteins. CD experiments were performed on Aviv 202 spectropolarimeter (Aviv Biomedical) with a 1 mm path length QS quartz sample cell at 25 °C. The CD spectra were recorded from 190 to 240 nm of wavelength with 1 nm resolution and 2 s of average time. PBS of pH 7.4 worked as blank to correct the baseline. Results were expressed as the molar mean residue ellipticity (θ) at a given wavelength.

Fluorescent probe binding assays

Fluorescent probe binding experiments were performed with 2 µM AegOBP22 solution in 50 mM PBS, pH 7.4. The fluorescent probe 1-NPN was purchased from Sigma-Aldrich (USA). The probe was dissolved in 10% v/v ETOH as 1 mM stock solution. To measure the affinity of the fluorescent probe 1-NPN to AegOBP22, the 2 µM AegOBP22 solution was titrated with aliquots of 1 mM 1-NPN solution to final concentrations of 2–16 µM 1-NPN. Spectra were recorded at 25 °C using a FluoroMax-3 spectrofluorometer (Jobin

Yvon SPEX, USA) with a 5-nm bandwidth for both excitation and emission. The excitation wavelength used for 1-NPN was 337 nm and emission spectra were recorded between 380 and 450 nm. Once the binding equilibrium has been reached, the relative proportion of probe bound to AegOBP22 was calculated by measuring fluorescent emission (expressed in arbitrary units). For determining dissociation constant (K_d), the intensity values corresponding to the maximum of fluorescent emission (407 nm) were plotted against total 1-NPN concentrations. K_d was obtained with a standard nonlinear regression method using Origin 8.0 software.

The ligand competitive binding assays aimed to displace the probe 1-NPN with competitive odors were performed with 2 μ M of AegOBP22a and 2 μ M 1-NPN, plus 4–24 μ M odors, respectively. Competitor concentrations causing a fluorescent decay to half-maximal intensity were taken as IC_{50} values. The apparent K_{diss} values were calculated as $K_{diss} = [IC_{50}] / (1 + [1-NPN] / K_d)$ with [1-NPN] being the free concentration of 1-NPN and K_d being the dissociation constant of the AegOBP22/1-NPN complex.

Results and discussion

AegOBP22 gene construction

Insect OBPs are very diverse proteins with an average of only 14% amino acid identity. In the studies of OBP motifs, these OBPs have been classified as ‘Classic’ OBPs, which have a highly conserved domain of six cysteine residues; ‘Plus-C’ OBPs, which have at least two extra conserved cysteines and a proline immediate after the sixth cysteine; ‘dimer’ OBPs, which contain two Classic OBP motifs in tandem; and ‘Atypical’ OBPs with an extended C-terminal region [8,18–22]. The majority of OBPs belong to the Classic subgroup with their six cysteines paired in three interlocked disulfide bridges forming a compact structure, consisting mainly of alpha-helical domains defining an internal binding pocket [21,23]. *A. aegypti* is identified to have 34 Classic OBPs, 17 Plus-C OBPs and 15 Atypical OBPs. The identified Classic OBPs of *A. aegypti* have an overall amino acid sequence similarity of 21.7%. Most of the 66 *A. aegypti* OBPs have a homolog in *A. gambiae* and similarities ranging from 16% to 63%. It is likely that these OBP genes evolved after the divergence of the two mosquito species *A. aegypti* and *A. gambiae* about 150 million years ago [21,24].

For better understanding of OBP structures and functions, one gene of Classic subgroup OBPs, AegOBP22 gene, was selected from GenBank (GenBank accession no. EAT42725) for recombinant protein expression. AegOBP22 has a homologue AgamOBP9 in *A. gambiae* and a homologue OBP99a in *D. melanogaster*. Considering the large scale of protein purification, an affinity tag, Strep-tag II, was added at N terminal of the AegOBP22 gene. Strep-tag II is a short peptide (8 amino acids, WSHPQFEK), which binds with high selectiv-

ity to Strep-Tactin, an engineered streptavidin [25,26]. For successful heterogeneity protein expression in *E. coli*, signal sequence is also a key factor. There are about 450 wild-type signal sequences for *E. coli* cell envelope proteins [<http://www.cf.ac.uk/biosi/staff-info/ehrmann/tools/ecce/signals.htm>]. In order to produce correctly folded proteins, signal sequence must be cleaved off by signal peptidases at the outer leaflet of *E. coli* inner membrane. At beginning, we selected some sequences from these 450 wild-type signal sequences as templates. By using computer software of signal sequence cleavage site prediction (see next paragraph), we found these templates did not have high cleavage probability at the end of the signal sequences. Hence, we made some mutant signal sequences from these templates, MNTLVTCLLGASLTVVA was one of these mutant signal sequences, it had a correct cleavage site. Unfortunately, it did not work. We did not detect AegOBP22 in cell pellets or in extracellular medium by Western blot analysis (First antibody was mouse monoclonal antibody/IgG1 specifications of StrepMAB-Classic, IBA cat. no. 2-1507-001. Secondary antibody for detection of StrepMAB-Classic was rabbit anti mouse pAb, horseradish peroxidase (HRP) conjugated, IBA cat. no. 2-1591-001). The failure could come from *E. coli* intracellular signal sequence recognition mechanism. Next, we chose a wild-type signal sequence of *E. coli* outer membrane protein, MKKTAIAIAVALAGFATVAQA is the signal sequence of OmpA, which is a monomeric β -barrel membrane protein. It is one of the major Omps of *E. coli* with \sim 100,000 copies/cell [27–29]. Its main function is to maintain structural integrity of the cell surface. We expected the high copy number in each cell will bring high secretory production. Moreover, by using cleavage site prediction tools, we found the wild-type signal sequence had a high cleavage probability at the end of the signal sequence. Finally, the AegOBP22 proteins were detected to exist abundantly in extracellular medium by Western blot analysis. The new recombinant protein gene is shown as Fig. 1.

Signal sequence cleavage site prediction

AegOBP22 cleavage site was predicted by using SignalP-NN tools and SignalP-HMM tools (<http://www.cbs.dtu.dk/services/SignalP/>). The SignalP-NN prediction result showed the most likely cleavage site was between positions 21 and 22 (in the middle of QA-AS) in AegOBP22 amino acid sequence. The SignalP-HMM result also showed the same cleavage position with a cleavage probability of 0.923 (Figure not shown).

Isoelectric point and MW prediction

By using program ProtParam (<http://ca.expasy.org/cgi-bin/prot-param>), the theoretical MW deduced from the AegOBP22 amino acid sequence beginning at ASWSH and ending at residues IKKDC was 15951.9 Da, while the predicted isoelectric point (pI) of

A	<i>NcoI</i>	<i>Start</i>					
	TACCATGGCC	ATGAAAAAAA	CGCAATTGC	AATTGCAGTT	GCACTGGCAG	GTTTGGCAAC	
	CGTGGCACAG	GCAGCTAGCT	GGTCACATCC	GCAGTTTGAA	AAAAGCTTGG	GCAGCGGTGA	
	ATTTACAGTT	AGCACCACCG	AAGACCTGCA	GCGTTATCGT	ACCGAATGTG	TTAGCAGCCT	
	GAAATATCCG	GCAGATTATG	TGGAAAAAAT	TAAAAAATGG	GAAATTTCCGG	AAGATGATAC	
	CACCATGTGC	TATATTAAT	GCGTGTTTAA	TAAAATGCAG	CTGTTTGATG	ATACCGAAGG	
	TCCGCTGGTT	GATAAATCTGG	TTCATCAGCT	GGCACATGGT	CGTGATGCAG	AAGAAGTTCCG	
	TACCGAAGTT	CTGAAATGCG	TGGATAAAAA	TACCGATAAT	AATGCATGCC	ATTGGGCATT	
	TCGTGGCTTT	AAATGCTTTC	AGAAAAATAA	TCTGAGCCTG	ATTAAGCCA	GCATTAATAA	
	AGATTGCTAA	TAACFCGAGC					
		<i>Stop</i>	<i>XhoI</i>				
	B	<i>Signal sequence</i>	<i>Streptag II</i>				
		MKKTAIAIAV	ALAGFATVAQ	AASWSHPQFE	KSLGSGEFTV	STTEDLQRYR	TECVSSLNIP
		ADYVEKFKKW	EFPEDDTTCM	YIKCVFNKMQ	LFDDTEGPLV	DNLVHQLAHG	RDAAEVRTEV
		LKCVDKNTDN	NACHWAFRGF	KCFQKNNLSL	IKASIKKDC*	*	

Fig. 1. The DNA (A) and corresponding amino acid (B) sequence of synthetic AegOBP22 gene. The gene was modified with N-terminal signal sequence and Strep-tag II from an *Aedes Egyptii* OBP22 gene (GenBank accession no. EAT42725). Translation start and stop sites as well as restriction cloning sites are indicated.

AeagOBP22 was 5.56. If the Strep-tag II sequence was not included, the theoretical MW of AeagOBP22 amino acid sequence beginning at SLGSG and ending at IKKDC was 14753.7 Da, corresponding pI was 5.36.

The prediction results show that AeagOBP22 has similar pI and MW to those of *A. gambiae* and *D. melanogaster*. The range of pIs for the dipteran OBPs is between 4 and 10, a wider range than that reported for the acidic pIs of lepidopteran OBPs. Thus the OBPs in the dipteran species can be positively or negatively charged at the physiological pH in insect antennae. The calculated MW of the AeagOBP22 is in agreement with the MWs of other insect OBPs. The MWs of the *A. aegypti* Classic OBPs are less than 15.5 kDa. Most of the Plus-C OBPs have MWs between 17 and 25 kDa and the Atypical OBPs have MWs between 25 and 35 kDa [21].

Protein purification and SDS-PAGE gel analysis

The Strep-Tactin column showed high binding affinity, the protein production was about 13 mg from per liter *E. coli* culture medium after Strep-Tactin elution process. In the second step of protein purification, AeagOBP22 proteins were purified by size-exclusion chromatography. The elution profile is shown in Fig. 2A. During gel filtration separations, recombinant AeagOBP22 protein samples were isolated in monomeric and dimeric forms, but the dimer production was far lower than monomer production, therefore we used only the monomeric form of the protein in subsequent studies. The final production of AeagOBP22 (including monomers and dimers) was about 5 mg pure proteins from per liter *E. coli* culture medium.

The samples eluted from the Strep-Tactin column were loaded on SDS-PAGE gel, the pH values of protein samples were 7.5, 8.0, 9.0 and 10.0. The SDS-PAGE gel shows AeagOBP22 MW is near 15 kDa, shown as Fig. 2B. The MW observed from SDS-PAGE gel is slightly lower than calculated MW. Two reasons may be responsible for this, one reason is the denature effect of surfactant SDS, which often makes small protein move faster than that in native gel; the other reason is the type of SDS-PAGE gel, although we used 10%–20% Tris Glycine gel, the protein band of AeagOBP22 almost ran to the bottom

of the gel. In this case, the accumulation errors are apparent. Choosing the gel with more high percentages of Tris Glycine could improve the precision. Fig. 2B shows that the AeagOBP22 production is the highest at pH 9.0, while the SDS-PAGE gel with two samples from monomer fractions of gel filtration shows most other proteins have been obviated, shown as Fig. 2C.

Mass spectrum analysis

Three sets of molar mass were obtained by LC-MS analysis. Electrospray mass spectrum and corresponding MW spectrum are shown in Fig. 3. The first set of molar mass was 14,574 Da (measured; while calculated MW was 14574.5 Da), corresponds to proteins beginning at STTED and ending at residues IKKDC. The second set of molar mass was 13,672 Da (measured; calculated, 13672.6 Da), corresponds to proteins beginning at GSGEF and ending at residues SLIKA. The third set of molar mass was 14,201 Da (measured; calculated, 14201.1 Da), corresponds to proteins beginning at KSLGS and ending at residues SLIKA. The difference between measured MW and calculated MW from mass spectrum data suggests that all six cysteine residues in AeagOBP22 are linked to form three disulfide bonds.

Secondary structure analysis

In Fig. 4A, the CD spectra show the secondary structures of AeagOBP22 at pH 5.0–9.0. The CD spectra exhibit a helical-rich protein profile with two minima at 208 and 225 nm. As the pH value decreases, the intensity of two minima increases, which suggests that the α -helix content of AeagOBP22 increases at low pH. A similar situation was occurred in silkworm PBPs; the protonation of acidic residues in its C-terminus at low pH triggered the formation of an additional α -helix, which occupied the binding pocket. In *A. gambiae* AgamOBP1, its α -helix content increased at low pH [3]. By contrast, the α -helix content of *Culex* mosquito CquiOBP1, a protein homologous to AgamOBP1, was reduced at low pH thus implying possible unwinding of α -helix structure at low pH [30]. From

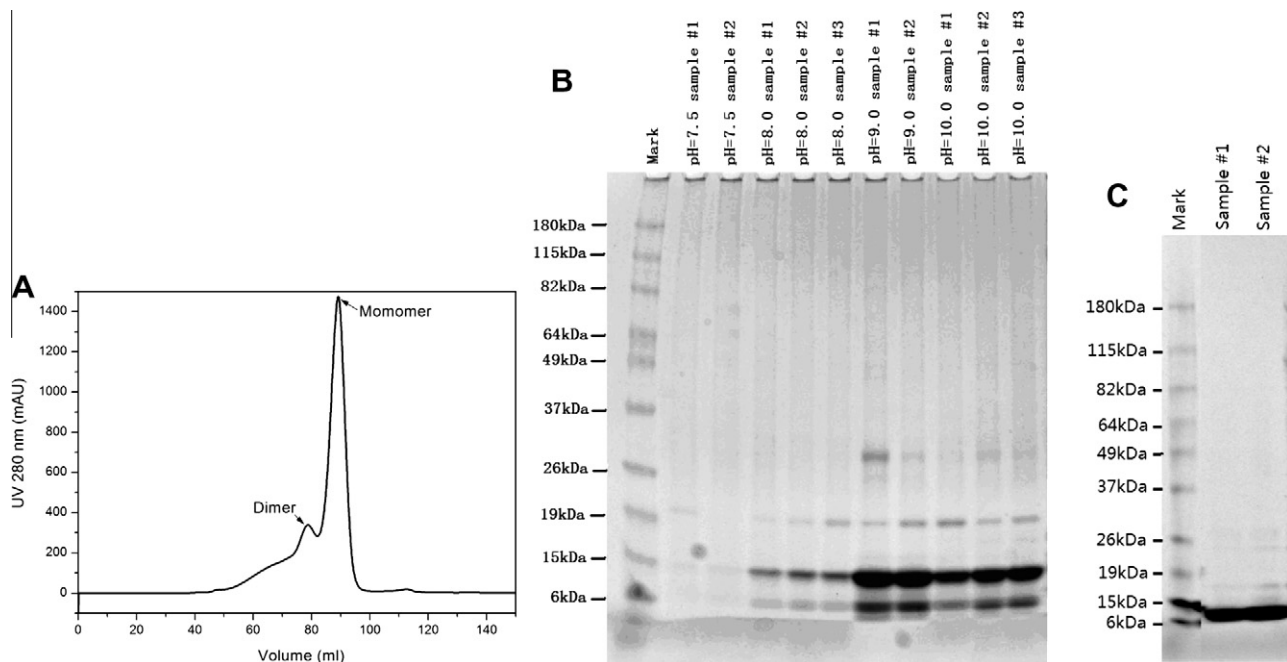


Fig. 2. (A) The elution profile of AeagOBP22 during gel filtration separations. (B) SDS-PAGE gel with samples obtained from Strep-Tactin elution fractions at pH 7.5–10.0. There were two or three samples of parallel test at each pH. The SDS-PAGE gel shows that the AeagOBP22 production is the highest at pH 9.0. The molecular weight of AeagOBP22 is near 15 kDa, the lane marked (Mark) shows molecular weight standards. (C) SDS-PAGE gel with two samples obtained from gel filtration monomer fractions.

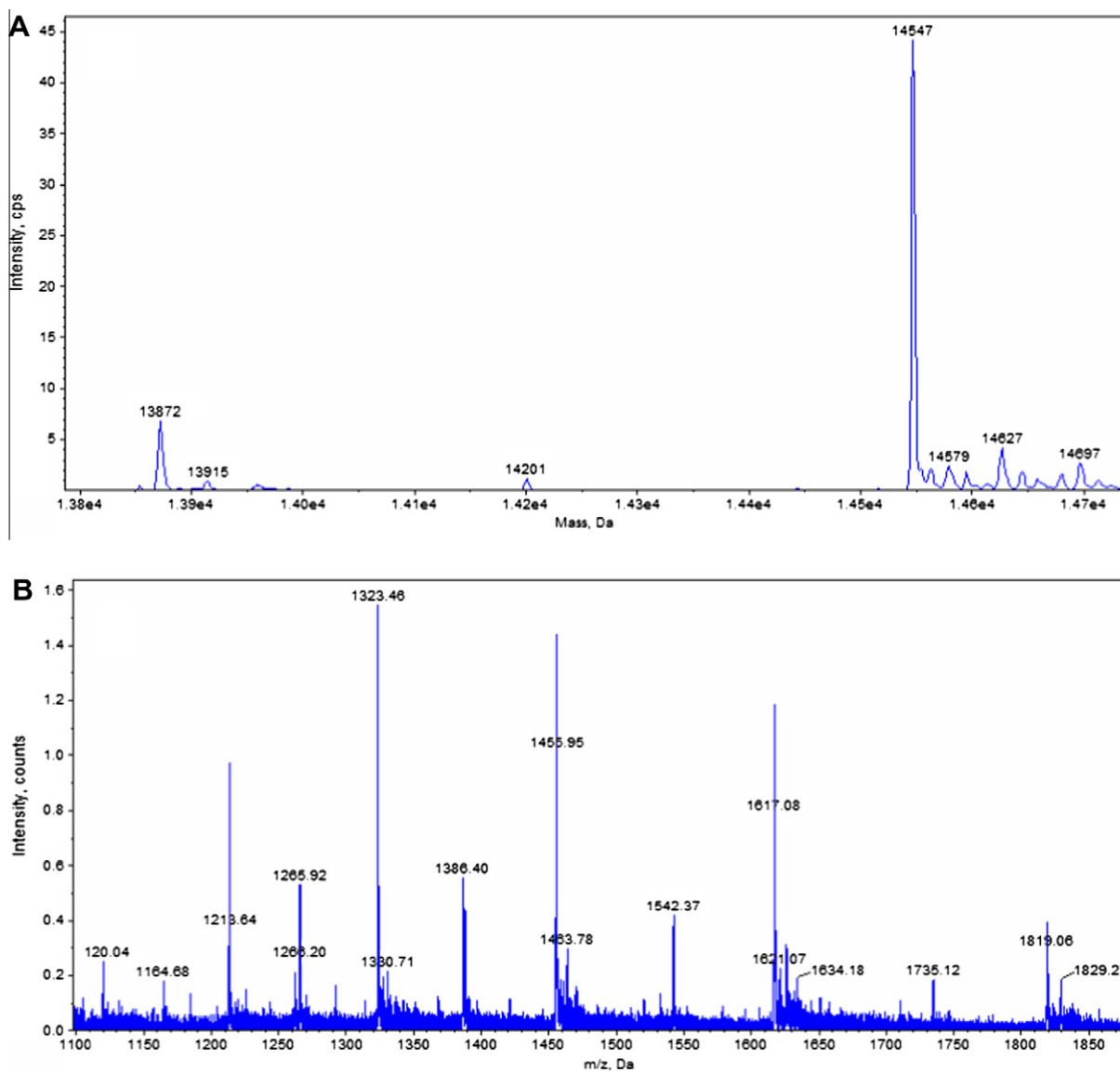


Fig. 3. Mass spectrometric data of purified AegOBP22 protein. (A) Electrospray mass spectrum and (B) corresponding molecular weight spectrum.

these we can see, even though these homologous OBPs have similar motifs, that they may have a different mechanism for pH-dependent odorant binding. Although how C-terminus plays the role is still not very clear in these OBPs, it is no doubt that the conformational change upon changing pH is associated with a loss of binding affinity of odors to these OBPs.

Fluorescent probe binding study

Fluorescent probe binding assay results are shown in Fig. 4. The fluorescent emission spectra were recorded at 25 °C of 2 μM 1-NPN in the presence of 2 μM AegOBP22 (solid squares); open circles indicate the fluorescence of probes alone (2 μM) and solid circles indicate protein solution alone (2 μM); excitation wavelength was 337 nm for 1-NPN, shown in Fig. 4B. The saturation curve of 1-NPN onto AegOBP22 (Fig. 4C) exhibits a dissociation constant K_d of 3.4 μM, showing the presence of a single type of binding site without any cooperativity effect.

The fluorescent intensity of the AegOBP22/1-NPN complexes is reduced with the increase of odorant concentration, while the de-

creased extent of ethyl vanillin is lesser than the other three odors; the curves are shown in Fig. 4D. The calculated apparent dissociation constants (K_{diss}), deduced from the half-maximal values (IC_{50}), are the highest for methyl benzoate and the lowest for cyclohexanone (Table 1). In any case, we notice that the ligand affinity for AegOBP22 correlates to the amount of fluorescent reduction, which reveals the displacement (d) of probes by odors.

Conclusion

Our study of producing AegOBP22 by using heterologous expression system proves *E. coli* extracellular secretion to be very useful way in obtaining correctly folded and active OBP proteins. Our work provides a new approach to study OBPs; it will enhance the understanding of mosquitoes' semiochemical system and helps to develop new disease control strategies against mosquitoes. Rapid advances along several research fronts have laid the foundation for a novel approach toward the design and development of a new generation of vector-borne disease control strategies. Moreover, our work will likely facilitate the design of bionic artificial nose

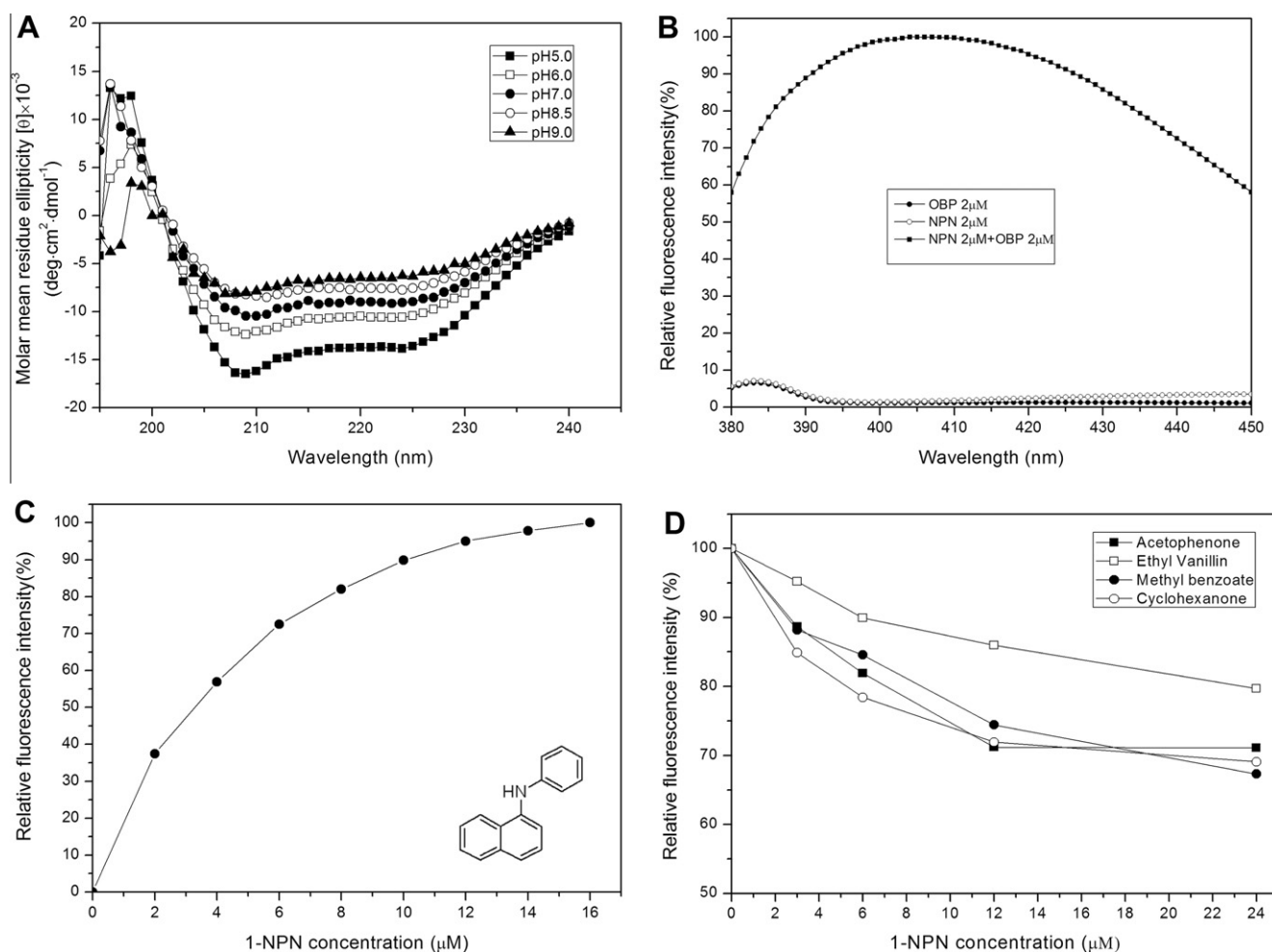
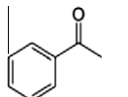
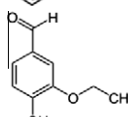
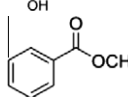
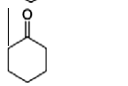


Fig. 4. CD spectra and 1-NPN fluorescent binding assays of AegOBP22. (A) The CD spectra of AegOBP22 at pH 5.0–9.0 show that two minima are around 208 and 222 nm, which are typical of a fold with a majority of α -helical secondary structures. (B) Fluorescent emission spectra recorded at 25 °C of 2 μM 1-NPN in the presence of 2 μM AegOBP22 (solid squares); open circles indicate the fluorescence of probes alone (2 μM) and solid circles indicate protein solution alone (2 μM); excitation wavelength was 337 nm. (C) Saturation binding curve of 1-NPN. The 2 μM AegOBP22 solution was titrated with aliquots of 1 mM solution of 1-NPN up to the final concentration of 16 μM . Using an excitation wavelength of 337 nm, emission spectra were recorded between 380 and 450 nm. Intensity values corresponding to the maximum of the peaks (407 nm) were plotted against total 1-NPN concentration. (D) Competitive binding assays of 1-NPN with several odors. Fluorescent intensity values of probe–protein complexes were assigned to 100% in the absence of competitor, and plotted against total ligand concentration, experimental conditions were as above. All spectra have been subjected to background subtraction.

Table 1
Affinity of ligands for AegOBP22 in competitive binding assays.

Ligands	Structure	d%	IC ₅₀	K _{diss}
Acetophenone		28.9	4.2	2.64
Ethyl vanillin		20.3	5.85	3.68
Methyl benzoate		32.7	6.3	3.97
Cyclohexanone		30.9	2.8	1.76

Note: Solution (2 μM) of the protein containing 2 μM 1-NPN were titrated with ligands to maximum concentrations of 24 μM . d, maximal percentage of displacement reached at high ligand concentration; IC₅₀, ligand concentration provoking a decay of fluorescence of half-maximal intensity; K_{diss}, apparent dissociation constant obtained by $K_{diss} = [\text{IC}_{50}] / (1 + [1\text{-NPN}] / K_d)$ with [1-NPN] for the free probe concentration and K_d the measured dissociation constants of OBP–probe complexes.

based on nano-bio devices for a wide range of applications, from detection of infinitesimal amounts of odors, emitted from diverse diseases and environment to develop artificial organs.

Acknowledgments

We acknowledge Prof. Luca Turin for stimulating and helpful discussions. G.Y. gratefully acknowledges the national CSC Foundation, China, for supporting his one-year visit to MIT in 2009.

References

- [1] Q.Y. Jiang, W.X. Wang, Z. Zhang, L. Zhang, Binding specificity of locust odorant binding protein and its key binding site for initial recognition of alcohols, *Insect. Biochem. Mol. Biol.* 39 (2009) 440–447.
- [2] J. Pelletier, A. Guidolin, Z. Syed, A.J. Cornel, W.S. Leal, Knockdown of a mosquito odorant binding protein involved in the sensitive detection of oviposition attractants, *J. Chem. Ecol.* 36 245–248.
- [3] M. Wogulis, T. Morgan, Y. Ishida, W.S. Leal, D.K. Wilson, The crystal structure of an odorant binding protein from *Anopheles gambiae*: evidence for a common ligand release mechanism, *Biochem. Biophys. Res. Commun.* 339 (2006) 157–164.
- [4] E. Andronopoulou et al., Specific interactions among odorant binding proteins of the African malaria vector *Anopheles gambiae*, *Insect Mol. Biol.* 15 (2006) 797–811.
- [5] H. Biessmann et al., The *Anopheles gambiae* odorant binding protein 1 (AgamOBP1) mediates indole recognition in the antennae of female mosquitoes, *PLoS One* 5 e9471.
- [6] F.R. Dani et al., Exploring proteins in *Anopheles gambiae* male and female antennae through MALDI mass spectrometry profiling, *PLoS One* 3 (2008) e2822.
- [7] S. Li, J.F. Picimbon, S. Ji, Y. Kan, Q. Chuanling, J.J. Zhou, P. Pelosi, Multiple functions of an odorant binding protein in the mosquito *Aedes aegypti*, *Biochem. Biophys. Res. Commun.* 372 (2008) 464–468.
- [8] J. Bohbot, R.G. Vogt, Antennal expressed genes of the yellow fever mosquito (*Aedes aegypti* L.); characterization of odorant binding protein 10 and takeout, *Insect Biochem. Mol. Biol.* 35 (2005) 961–979.
- [9] Z. Syed, W.S. Leal, Mosquitoes smell and avoid the insect repellent DEET, *Proc. Natl. Acad. Sci. USA* 105 (2008) 13598–13603.
- [10] J.P. Andersen, A. Schwartz, J.B. Gramsbergen, V. Loeschcke, Dopamine levels in the mosquito *Aedes aegypti* during adult development, following blood feeding and in response to heat stress, *J. Insect Physiol.* 52 (2006) 1163–1170.
- [11] S. Thangamani, S.K. Wikel, Differential expression of *Aedes aegypti* salivary transcriptome upon blood feeding, *Parasit Vectors* 2 (2009) 34.
- [12] H. Breer, Olfactory receptors: molecular basis for recognition and discrimination of odors, *Anal. Bioanal. Chem.* 377 (2003) 427–433.
- [13] L. Briand et al., Evidence of an odorant binding protein in the human olfactory mucus: location, structural characterization, and odorant binding properties, *Biochemistry* 41 (2002) 7241–7252.
- [14] L.J. Zwiebel, W. Takken, Olfactory regulation of mosquito–host interactions, *Insect Biochem. Mol. Biol.* 34 (2004) 645–652.
- [15] X. Jin et al., Expression and immunolocalisation of odorant binding and chemosensory proteins in locusts, *Cell Mol. Life Sci.* 62 (2005) 1156–1166.
- [16] E. Lescop, L. Briand, J.C. Pernollet, E. Guittet, Structural basis of the broad specificity of a general odorant binding protein from honeybee, *Biochemistry* 48 (2009) 2431–2441.
- [17] C. Nespoulous, L. Briand, M.M. Delage, V. Tran, J.C. Pernollet, Odorant binding and conformational changes of a rat odorant binding protein, *Chem Senses* 29 (2004) 189–198.
- [18] V. Nene et al., Severson, Genome sequence of *Aedes aegypti*, a major arbovirus vector, *Science* 316 (2007) 1718–1723.
- [19] J. Pelletier, W.S. Leal, Genome analysis and expression patterns of odorant binding proteins from the Southern House mosquito *Culex pipiens quinquefasciatus*, *PLoS One* 4 (2009) e6237.
- [20] C.T. Smartt, J.S. Erickson, Expression of a novel member of the odorant binding protein gene family in *Culex nigripalpus* (Diptera: Culicidae), *J. Med. Entomol.* 46 (2009) 1376–1381.
- [21] J.J. Zhou, X.L. He, J.A. Pickett, L.M. Field, Identification of odorant binding proteins of the yellow fever mosquito *Aedes aegypti*: genome annotation and comparative analyses, *Insect Mol. Biol.* 17 (2008) 147–163.
- [22] J.J. Zhou, W. Huang, G.A. Zhang, J.A. Pickett, L.M. Field, “Plus-C” Odorant binding protein genes in two *Drosophila* species and the malaria mosquito *Anopheles gambiae*, *Gene* 327 (2004) 117–129.
- [23] N.R. Leite, R. Krogh, W. Xu, Y. Ishida, J. Iulek, W.S. Leal, G. Oliva, Structure of an odorant binding protein from the mosquito *Aedes aegypti* suggests a binding pocket covered by a pH-sensitive “Lid”, *PLoS One* 4 (2009) e8006.
- [24] J. Krzywinski, O.G. Grushko, N.J. Besansky, Analysis of the complete mitochondrial DNA from *Anopheles funestus*: an improved dipteran mitochondrial genome annotation and a temporal dimension of mosquito evolution, *Mol. Phylogenet. Evol.* 39 (2006) 417–423.
- [25] J.D. Hirsch, L. Eslamizar, B.J. Filanoski, N. Malekzadeh, R.P. Haugland, J.M. Beechem, Easily reversible desthiobiotin binding to streptavidin, avidin, and other biotin-binding proteins: uses for protein labeling, detection, and isolation, *Anal. Biochem.* 308 (2002) 343–357.
- [26] T.G. Schmidt, A. Skerra, The Strep-tag system for one-step purification and high-affinity detection or capturing of proteins, *Nat. Protoc.* 2 (2007) 1528–1535.
- [27] S.C. Chang, M.H. Su, Y.H. Lee, Roles of the signal peptide and mature domains in the secretion and maturation of the neutral metalloprotease from *Streptomyces cacaoi*, *Biochem. J.* 321 (Pt. 1) (1997) 29–37.
- [28] J.H. Choi, S.Y. Lee, Secretory and extracellular production of recombinant proteins using *Escherichia coli*, *Appl. Microbiol. Biotechnol.* 64 (2004) 625–635.
- [29] A. Kuhn, D. Kiefer, C. Kohne, H.Y. Zhu, W.R. Tschantz, R.E. Dalbey, Evidence for a loop-like insertion mechanism of pro-Omp A into the inner membrane of *Escherichia coli*, *Eur. J. Biochem.* 226 (1994) 891–897.
- [30] W.S. Leal et al., Reverse and conventional chemical ecology approaches for the development of oviposition attractants for *Culex* mosquitoes, *PLoS One* 3 (2008) e3045.